

# Temporal and phase measurements of ultraviolet femtosecond pulses at 200 nm by molecular alignment based frequency resolved optical gating

Hao Li, Jia Liu, Yahui Feng, Cheng Chen, Haifeng Pan, Jian Wu, and Heping Zeng<sup>a)</sup>

State Key Laboratory of Precision Spectroscopy, East China Normal University, Shanghai 200062, China

(Received 17 October 2010; accepted 16 June 2011; published online 8 July 2011)

We demonstrate that the temporal profile and phase of a weak ultraviolet femtosecond pulse around 200 nm can be measured by molecular alignment based cross-correlation frequency resolved optical gating technique. This technique employs the impulsive alignment of gaseous molecules as gate function and exhibits the advantage of no phase-matching constraint and applicability to pulses at various wavelengths. Simultaneous measurements of near-infrared and ultraviolet pulses are demonstrated. Its agreements with the independent spectral phase interferometry for direct electric field reconstruction and second-order auto-correlation measurements confirm that the molecular alignment gating is a robust technique for ultrashort pulse diagnosis. © 2011 American Institute of Physics. [doi:10.1063/1.3609238]

The ultraviolet (UV) light pulse, for its high single-photon energy and high spectral resolution, has been widely used in ultrafast optics, chemistry, and biology.<sup>1,2</sup> In many cases, the temporal profiles of the UV pulses are concerned. Taking the measurement of a weak UV pulse around 200 nm as an example, if the well-developed method of second harmonic generation (SHG) frequency resolved optical gating (FROG) (Ref. 3) is used, an efficient nonlinear optical crystal for SHG to produce signal at 100 nm is required, which goes beyond the transparent windows of the mostly used nonlinear optical crystals. The nonlinear frequency down conversion cross-correlation FROG (XFROG) with an intense near-infrared reference pulse is an alternative approach for UV pulse measurement,<sup>4</sup> which is somehow affected by the phase-matching between the light waves of different wavelengths. On the other hand, the phase-matching constraint could be avoided by the polarization-gated FROG (PG-FROG) technique,<sup>3,5,6</sup> where a cubic nonlinear medium is usually used to produce a gate function. Two-photon absorption autocorrelation<sup>7</sup> was also demonstrated to be effective to measure UV pulse without phase-matching constraint.

In this paper, we demonstrate that a weak UV pulse around 200 nm can be fully characterized by the molecular alignment gated XFROG (M-XFROG) in air. The M-XFROG utilizes the transient birefringence effect induced by the impulsive alignment of air molecules, which actually relies on a linear optical gating process without phase-matching constraint on the spectral range or bandwidth. Furthermore, the M-XFROG is used to simultaneously measure pulses of different wavelengths and distinguish the relative time delay between them. As compared with the PG-FROG where cubic nonlinear media are usually used, the gate function for the M-XFROG is produced by transiently aligned gaseous molecules.

The linear molecules with polarizability difference  $\Delta\alpha$  between the components parallel and perpendicular to the molecular axis experiences a torque during its dipole interaction with the applied laser field, which enforces the molecules to be aligned along the laser field polarization.<sup>8</sup> The quantum beatings of the impulsively pre-excited rotational

wavepackets result in periodic molecular alignment with the molecular axis parallel or perpendicular to the laser field polarization. The pre-aligned molecules show an orientation-dependent refractive index, resulting in an observable time-dependent change of the polarization state of a properly matched target pulse. We recently demonstrated that this transient wave-plate worked as a gate function could be used to measure ultrashort laser pulses based on the M-XFROG (Refs. 9 and 10) and to get periodic revivals of ultrafast optical imaging.<sup>11</sup> Here, we further show that the ultrashort UV pulse around 200 nm can be fully characterized by using the M-XFROG in air and demonstrate the possibility to simultaneously measure pulses of different wavelengths.

To demonstrate the measurement of ultrashort UV pulse at 200 nm by the M-XFROG, we performed experiments as schematically illustrated in Fig. 1. The output from an amplified Ti:Sapphire laser system ( $\sim 50$  fs, 800 nm, 1 kHz) was split into two parts with an energy ratio of 1:2. One part was used to align the air molecules (M-pulse), and the other part was used to generate the target UV pulse. To produce the 200 nm target pulse, we first 2:1 down-collimated the fundamental wave (FW) beam by the convex ( $f=30$  cm) and concave ( $f=-15$  cm) lens and frequency-doubled the FW pulse in a  $\beta$ -barium boron oxide (BBO) crystal (type I,  $29.2^\circ$  cut,  $100\text{-}\mu\text{m}$  thick). We then used a second  $\beta$ -BBO crystal (type-II,  $55.4^\circ$ -cut,  $100\text{-}\mu\text{m}$  thick) to generate a third-harmonic (TH)

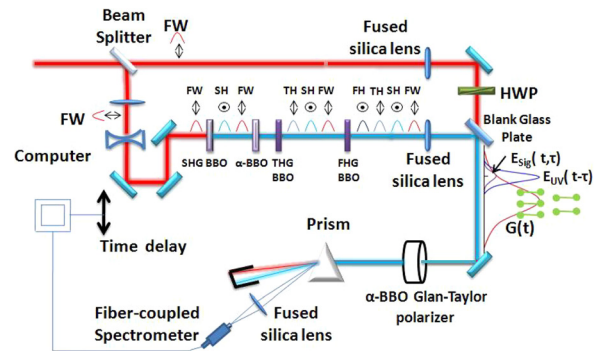


FIG. 1. (Color online) (a) The experimental setup. HWP: half wave plate at 800 nm. The s and p polarizations of the harmonic waves are indicated by the circular-dots and arrows, respectively.

<sup>a)</sup>Electronic mail: hpzeng@phy.ecnu.edu.cn.

pulse by frequency-summing the residual FW and SH pulses. In order to improve the TH generation efficiency, the group velocity mismatching between the orthogonally polarized FW and SH pulse was compensated by inserting a 0.5-mm-thick  $\alpha$ -BBO crystal, which acted as a birefringence plate with its fast and slow axes orientated along the polarizations of the SH and FW pulses, respectively. The generated TH and residual FW pulses were then sent to a third  $\beta$ -BBO crystal (type I, 64.8°-cut, 100- $\mu$ m thick) to generate a fourth harmonic (FH) pulse around 200 nm by frequency-summing process. The polarizations of the pulses were labeled in Fig. 1, where the s and p polarizations of the fundamental and harmonic waves are indicated by the circular-dots and arrows, respectively.

The M-pulse at 800 nm and generated UV target pulse around 200 nm were focused by two separated convex lenses of  $f = 40$  and 25 cm, respectively, and collinearly combined with a blank glass plate which partly reflected and transmitted UV pulse and M-pulse. The positions of the lenses were adjusted so that their foci were overlapped in the interaction region. The energy of the M-pulse was measured to be  $\sim 300 \mu\text{J}$  after the combining glass plate and its intensity at the focus was estimated to be  $\sim 1 \times 10^{13} \text{ W/cm}^2$ , which was proper for aligning air molecules. The UV pulse around 200 nm was so weak that it could be seen only with a fluorescence card and impossible to be measured by our power-meter. After a high quality  $\alpha$ -BBO Glan-Taylor polarizer (extinction ratio is  $\sim 1 \times 10^{-5}$  for  $\sim 200$  nm pulse) and a fused silica prism, the UV pulse around 200 nm was focused into a fiber-coupled spectrometer (HR4000, Ocean Optics) with a fused silica lens ( $f = 10$  cm) for M-XFROG trace measurement. The transmission direction of the polarizer was set to be perpendicular to the incident UV pulse, so that only the components with rotated polarization were measured. For the well-defined linear polarization of the UV pulse ensured by the phase matching condition during its generation, no polarizer was used before its interaction with the molecular alignment gate. A high signal-to-noise ratio of the FROG trace was obtained by subtracting the measured background (without M-pulse) from the measured spectra (with M-pulse) before retrieving. The time delay of the target pulse was controlled by a motorizing translation stage with a step of 5 fs. At each delay, the spectrum was averaged over  $\sim 150$  pulses. In order to optimize the measured signal, the polarization of the FW M-pulse was rotated to be 45° with respect to the target UV pulse by using an 800-nm half-wave plate. Here, we used the first molecular alignment signal of the pre-aligned air molecules of  $\text{N}_2$  and  $\text{O}_2$  as the gate function for the M-XFROG trace measurement. We used air because of its wide availability and convenience of experimental performance, which could readily be replaced by other molecular gases. Note that the absorption of UV pulses is typically unavoidable in most FROG or other pulse measurement techniques performed in non-vacuum media. In the retrieval of the target UV pulse from the measured M-XFROG trace, the spectrum distortion due to the absorption of oxygen and the polarizer was corrected according to the absorption characteristics of oxygen<sup>12</sup> and the  $\alpha$ -BBO polarizer<sup>13</sup> around 200 nm. This gave a slight calibration to the retrieved UV pulse for its narrow spectral bandwidth. The transmission range of  $\alpha$ -BBO from 190 to 3500 nm<sup>13,14</sup> allowed us to measure the FH pulse around 200 nm. Instead of the relative phase, only the intensity profile of the polarization-rotated components of the target pulse was recorded

by the spectrometer as a function of the time delay between the target pulse and the transient gate. Since the  $\alpha$ -BBO polarizer was placed after the interaction region (defined as the region where molecules were significantly aligned), its dispersion produced negligible influence on the XFROG measurement. The generalized projections iterative algorithm<sup>3,5</sup> was used to retrieve the envelope and phase of the target pulse. The iterative process was repeated until the trace error reached a proper level.<sup>3</sup>

Figures 2(a) and 2(b) show the measured and retrieved M-XFROG trace of the UV pulse around 200 nm with an error of  $\sim 5.2 \times 10^{-4}$  after 400 iterations. The retrieved temporal profile and phase are presented in Fig. 2(c). As shown in Fig. 2(c), the temporal duration of the UV pulse around 200 nm is about  $\sim 44$  fs (full width at half maximum, FWHM), which shows a little positive chirp according to the retrieved phase. The gate function plays a critical role in the pulse retrieval. Figure 2(d) shows the retrieved gate function by using the twin retrieval of excitation electric fields frequency resolved optical gating (TREFROG) algorithm.<sup>15</sup> Both the gate function and target pulse were simultaneously reconstructed from the measured XFROG trace. It agrees well with the measured molecular alignment signal.

Since no phase matching was required for the M-XFROG, it could be used for simultaneous measurements of two or more pulses centered at different wavelengths. In our experiment, along with the FH pulse around 200 nm, there were FW ( $\sim 800$  nm), SH ( $\sim 400$  nm), and TH ( $\sim 267$  nm) pulses as well. As indicated in Fig. 1, the SH and FH pulses had the same polarization, while the FW and TH pulses had the same polarization. Since the same polarized pulses experienced similar polarization rotation by the molecular alignment gate, we then tried to simultaneously measure the FW and TH pulses by the M-XFROG technique. There were some adjustments on the experimental setup as shown in Fig. 1. First, the dispersion prism was removed. Second, in order to remove the influence of the FW M-pulse on the measurement of the FW target pulse, we slightly crossed the M-pulse and target pulses at a small angle ( $\sim 5^\circ$ , the foci still overlapped with each other at the crossing point) so that only the FW and TH target pulses were detected by the spectrometer. The M-pulse energy was  $\sim 300 \mu\text{J}$  after combining plate and the energies of the FW and TH target pulses were  $\sim 10$  and  $\sim 3 \mu\text{J}$ , respectively. The transmission direction of the polarizer was reset to be perpendicular to the polarizations of target pulses.

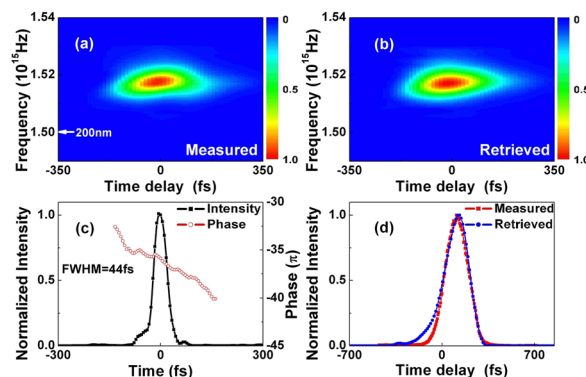


FIG. 2. (Color online) (a) The measured and (b) the retrieved M-XFROG traces of the FH pulse around 200 nm. (c) The retrieved pulse intensity (black squared-curve) and phase (red circled-curve). (d) The measured molecular alignment signal (red square-curve) and the retrieved gate function (blue circle-curve).

Figure 3(a) shows the simultaneously measured M-XFROG traces of the FW and TH target pulses for one XFROG measurement, which located in different spectral and temporal ranges. The relative delay between the FW and TH FROG traces was consistent with the fact that the FW pulse propagates faster than the TH pulse in the normally dispersive media. The retrieved TH and FW XFROG traces (with errors of  $\sim 4.0 \times 10^{-4}$  and  $\sim 2.2 \times 10^{-4}$  after 400 iterations, respectively), temporal profiles are illustrated in Figs. 3(b)–3(e), which show that the FWHM durations of the TH and FW pulses are about  $\sim 54$  and  $\sim 64$  fs, respectively. Because of the  $5^\circ$  crossing angle between the M-pulse and target pulse, there existed a time smearing<sup>16</sup> about 0.75 fs for the measured pulse duration. This clearly demonstrated the M-XFROG technique could be useful for the simultaneous measurements of pulses at different wavelengths,<sup>17</sup> which also precisely distinguished the relative delay between different pulses.

Finally, the reliability of the M-XFROG was confirmed by comparing it with the measurements of second-order auto-correlation and spectral phase interferometry for direct electric field reconstruction (SPIDER). Here, test pulses at 800 nm were independently characterized by the M-XFROG, auto-correlation and SPIDER measurements. The measured and retrieved M-XFROG traces are shown in Figs. 4(a) and 4(b), respectively. The red solid curve in Fig. 4(c) shows the retrieved intensity profile of the test pulse (FWHM  $\sim 47$  fs, the error is  $\sim 1.12 \times 10^{-3}$  after 400 iterations), which agreed well with the one retrieved from the SPIDER measurement (blue dashed curve, FWHM  $\sim 49$  fs, APE SPIDER). Figure 4(d) shows the reconstructed auto-correlation traces from the M-XFROG (red solid curve, FWHM  $\sim 67$  fs) and SPIDER (blue dashed curve, FWHM  $\sim 71$  fs) measurements, which agrees well with the directly measured second-order auto-

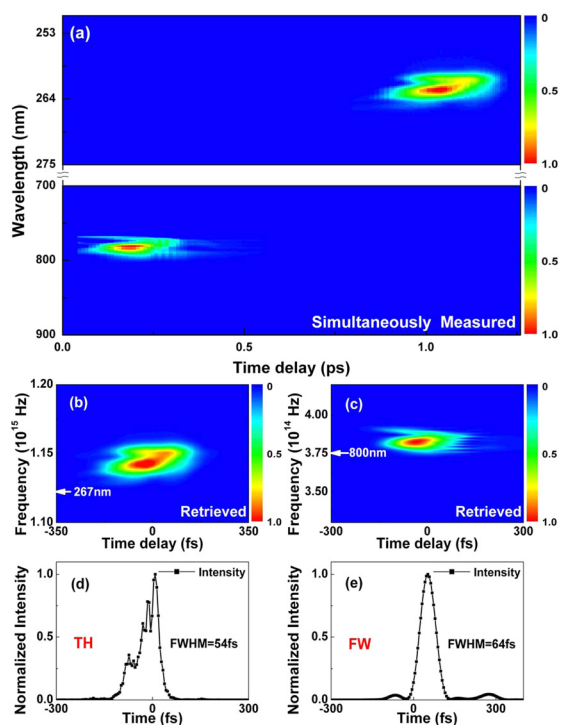


FIG. 3. (Color online) (a) The simultaneously measured M-XFROG traces of the FW and TH pulses. The retrieved (b), (c) M-XFROG traces and (d), (e) temporal profiles of the TH and FW pulses.

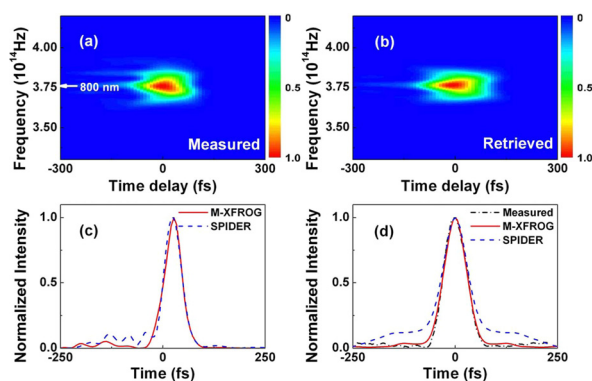


FIG. 4. (Color online) (a) The measured and (b) retrieved M-XFROG traces. (c) The retrieved intensity profiles of the target pulse based on the M-XFROG (red solid curve) and SPIDER (blue dashed curve) measurements. (d) The measured second-order auto-correlation signal (black dash-dotted curve) and the reconstructed ones based on the M-XFROG (red solid curve) and SPIDER (blue dashed curve) measurements.

correlation signal (black dash-dotted curve, FWHM  $\sim 69$  fs). The FWHM of the auto-correlation signal is about 1.4 times of that of the corresponding intensity profile, indicating the near Gaussian shape of the test pulse. Benefiting from the cross-correlation essential, the M-XFROG can be used to measure ultrashort pulse with duration smaller than the gate width. It was experimentally demonstrated that the M-XFROG could be used to measure few-cycle pulse of  $\sim 12.8$  fs.<sup>10</sup>

In summary, we have demonstrated that weak UV pulses around 200 nm could be fully characterized by the M-XFROG with the pre-aligned molecules in air as the gate function. Simultaneous measurements of two pulses at different wavelengths (near-infrared and UV) was also presented, where their relative time delay could be precisely determined. The validity of the M-XFROG technique was confirmed by comparing it with independent SPIDER and second-order auto-correlation measurements.

This work was partly funded by National Natural Science Fund (10525416 and 10804032) and National Key Project for Basic Research (2011CB808105).

- <sup>1</sup>I. V. Hertel and W. Radloff, *Rep. Prog. Phys.* **69**, 1897 (2006).
- <sup>2</sup>S. A. Trushin, W. E. Schmid, and W. Fuß, *Chem. Phys. Lett.* **468**, 9 (2008).
- <sup>3</sup>R. Trebino, K. W. DeLong, D. N. Fittinghoff, J. N. Sweetser, M. A. Krubgel, and B. A. Richman, *Rev. Sci. Instrum.* **68**, 3277 (1997).
- <sup>4</sup>S. Linden, J. Kuhl, and H. Giessen, *Opt. Lett.* **24**, 569 (1999).
- <sup>5</sup>K. W. DeLong, R. Trebino, and D. J. Kane, *J. Opt. Soc. Am. B* **11**, 1595 (1994).
- <sup>6</sup>B. Kohler, V. V. Yakovlev, K. R. Wilson, J. Squier, K. W. DeLong, and R. Trebino, *Opt. Lett.* **20**, 483 (1995).
- <sup>7</sup>A. M. Streltsov, J. K. Ranka, and A. L. Gaeta, *Opt. Lett.* **23**, 798 (1998).
- <sup>8</sup>H. Stapelfeldt and T. Seideman, *Rev. Mod. Phys.* **75**, 543 (2003).
- <sup>9</sup>P. Lu, J. Liu, H. Li, H. Pan, J. Wu, and H. Zeng, *Appl. Phys. Lett.* **97**, 061101 (2010).
- <sup>10</sup>J. Liu, Y. Feng, H. Li, P. Lu, H. Pan, J. Wu, and H. Zeng, *Opt. Express* **19**, 40 (2011).
- <sup>11</sup>J. Wu, P. Lu, J. Liu, H. Li, H. Pan, and H. Zeng, *Appl. Phys. Lett.* **97**, 161106 (2010).
- <sup>12</sup>L. P. Granath, *Phys. Rev.* **34**, 1045 (1929).
- <sup>13</sup>Z. Guoqing, X. Jun, C. Xingda, Z. Heye, W. Siting, X. Ke, D. Peizhen, and G. Fuxi, *J. Cryst. Growth* **191**, 517 (1998).
- <sup>14</sup>K. Kokh and A. Kokh, *J. Cryst. Growth* **317**, 1 (2011).
- <sup>15</sup>K. W. DeLong, R. Trebino, and W. E. White, *J. Opt. Soc. Am. B* **12**, 2463 (1995).
- <sup>16</sup>A. Baltuska, M. S. Pshenichnikov, and D. A. Wiersma, *Opt. Lett.* **23**, 1474 (1998).
- <sup>17</sup>R. Weigand, J. T. Mendonça, and H. M. Crespo, *Phys. Rev. A* **79**, 063838 (2009).